From Lithium to Proton Mobility in Garnet Electrolytes: An NMR and Conductivity Study of $H_{5.2}Li_{1.3}La_3Zr_{1.5}Ta_{0.5}O_{12}$

Florian Stainer[1], Junji Akimoto[2], Yoshitaka Matsushita[2], Kazutaka Mitsuishi[2],

Kazunori Takada[2], and H. Martin R. Wilkening[1]*

[1] Graz University of Technology, Institute of Chemistry and Technology of Materials (NAWI Graz), Stremayrgasse 9, 8010 Graz, Austria

[2] National Institute for Materials Science (NIMS), Tskuba, Ibaraki 305-0044, Japan

* corresponding author: wilkening@tugraz.at

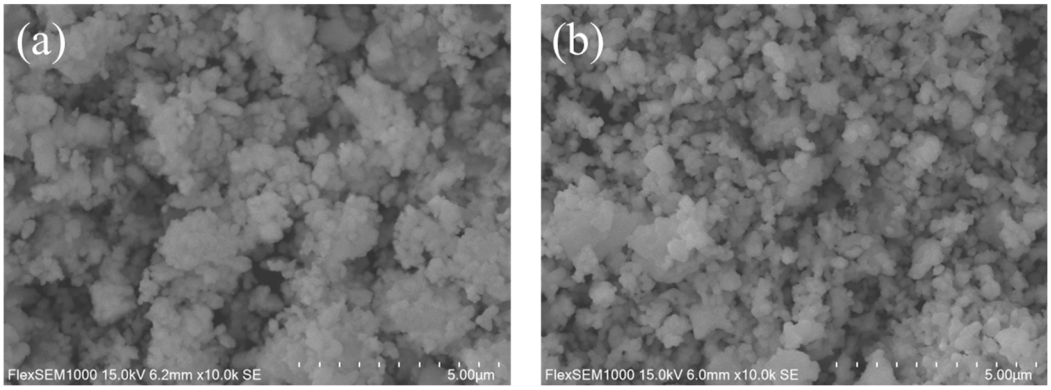

Figure S1: SEM images of (a) the parent $Li_{6.5}La_3Zr_{1.5}Ta_{0.5}O_{12}$ garnet sample and (b) the Li^+/H^+ ion-exchanged polycrystalline $H_{5.20}Li_{1.30}La_3Zr_{1.5}Ta_{0.5}O_{12}$ sample.

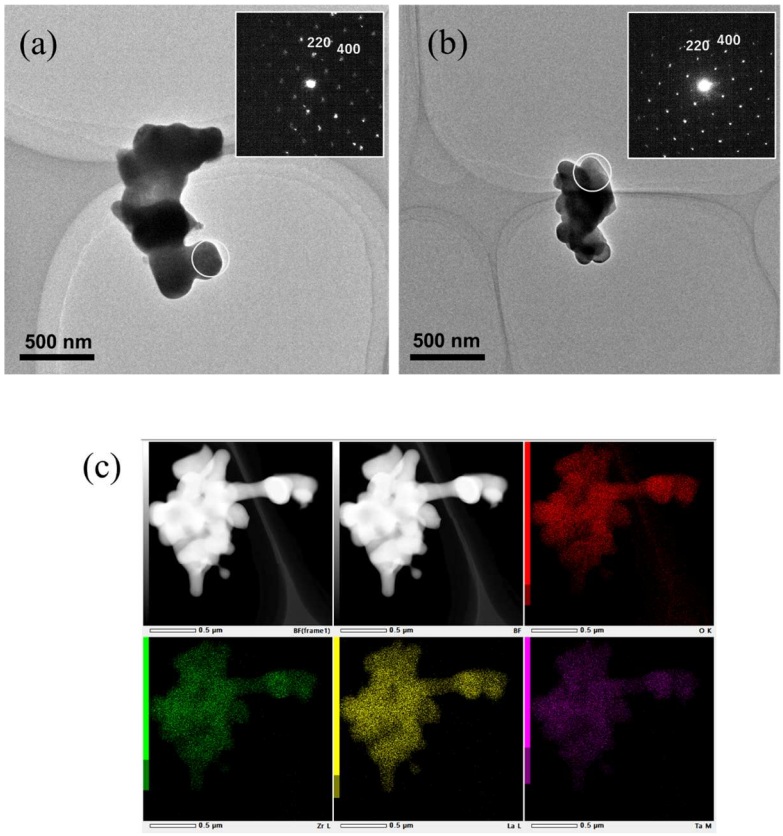

Figure S2: TEM images of (a) LLZTO and (b) HLZTO powder samples, as well as (c) the corresponding energy-dispersive X-ray spectroscopy (EDS) elemental maps of the LLZTO sample, acquired using a JEOL JEM-ARM200F aberration-corrected electron microscope operated at 200 kV.

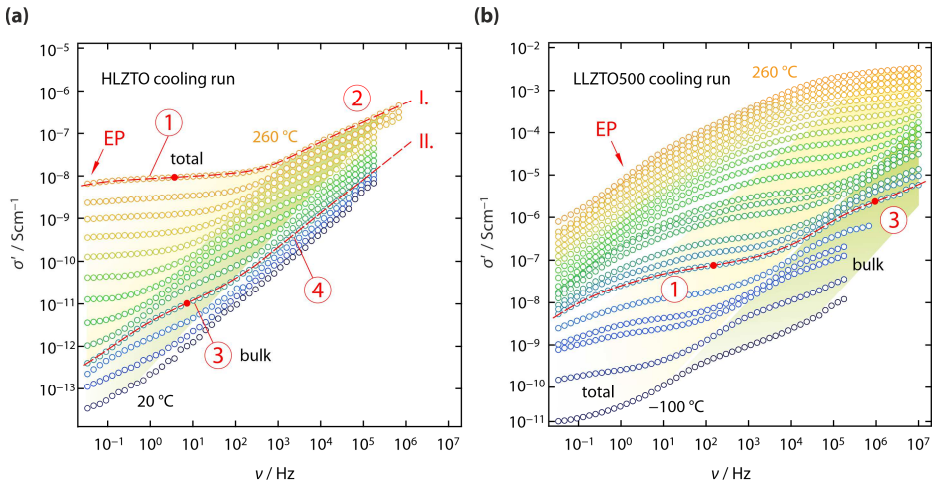

Figure S3: Conductivity isotherms, real part of the complex conductivity σ' versus frequency, of HLZTO (a) and LLZTO500 (b). Both datasets show a narrow bulk plateau (3) and a broader grain-boundary plateau (total conductivity, (1)), similar to the situation discussed for Li-bearing titanium phosphates.[1] The isotherms in both panels were recorded during cooling from 260 °C down to temperatures as low as – 100 °C. EP denotes electrode polarization. Regions (2) and (4) mirror the dispersive parts of the DC "plateaus" (1) and (3). The dashed lines serve as a guide to the eye, helping to visualize how the spectral shape changes when going from high to lower temperatures. Line I. in panel (a) shows a pronounced DC plateau at low frequencies, followed by a region influenced by both dispersive processes and bulk contributions. The latter becomes more apparent at lower temperatures, as illustrated by isotherm II. in panel (a). In panel (b), corresponding to LLZTO500, the two contributions are clearly better resolved, making their separation more straightforward, although still not as ideal as in other cases.[2] The corresponding Nyquist plots are dominated by the grain-boundary response, while the bulk contributions are much less visible.

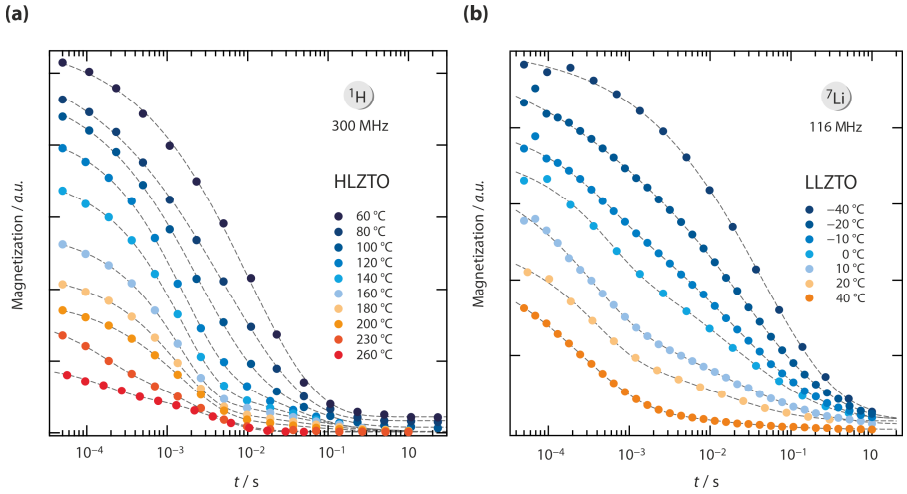

Figure S4: (a) ^{1}H NMR $R_{1\rho}$ transients from the first heating run of HLZTO, showing the emergence of a second, slower relaxation process at elevated temperatures. The data allow an estimate of the relative contributions of the two processes. Between 80 and 200 °C, the slower component (longer relaxation time) accounts for only a minor fraction of the total relaxation. At 230 and 260 °C, both components shift to substantially shorter relaxation times, and the relative weight of the slower process increases markedly. (b) ^{7}Li NMR SLR transients of LLZTO. Between −20 °C and 40 °C, the transients are double-exponential. With increasing temperature, the relative contribution of the slower component decreases. We interpret these components as reflecting populations of spins with different diffusivities, analogous to the behaviour observed in ^{1}H NMR, rather than as a consequence of the spin-3/2 nature of the ^{7}Li nucleus.

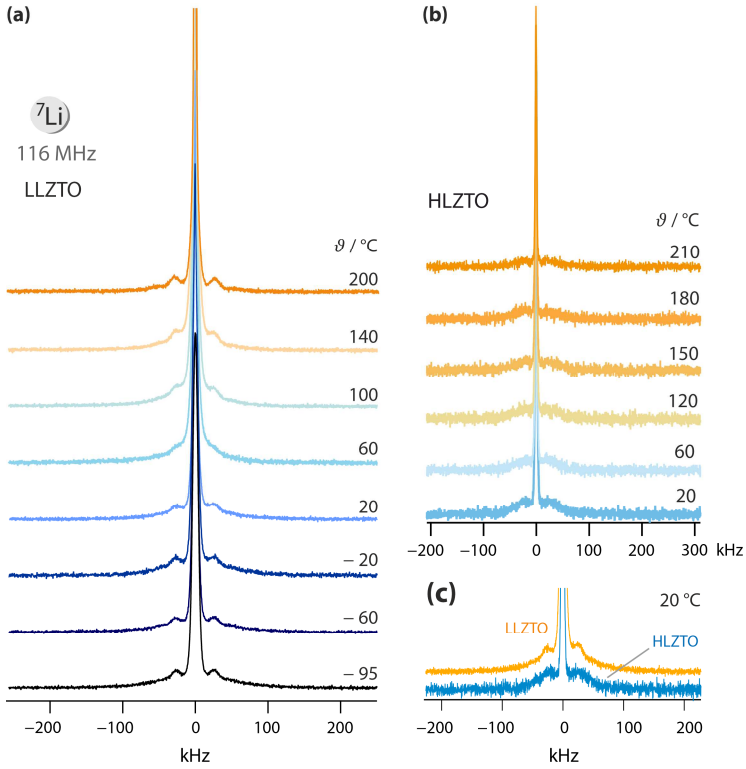

Figure S5: Static ^{7}Li (spin quantum number I = 3/2) NMR spectra of LLZTO (a) and HLZTO (b, c), shown over the full frequency range to highlight the quadrupolar contributions visible as singularities flanking the central line. For LLZTO, starting at 20 °C, and more distinctly at 60 °C, the original quadrupolar pattern becomes smeared and then reappears with a slightly modified line shape but an almost unchanged quadrupole coupling constant, as evidenced by the preserved 90° singularities when the pattern is described by an axially symmetric electric field gradient. These changes indicate that, with increasing temperature, the ions gain access to additional diffusion pathways.[3] In HLZTO, the quadrupole foot is significantly weaker, see also (c), and vanishes at temperatures above 210 °C.

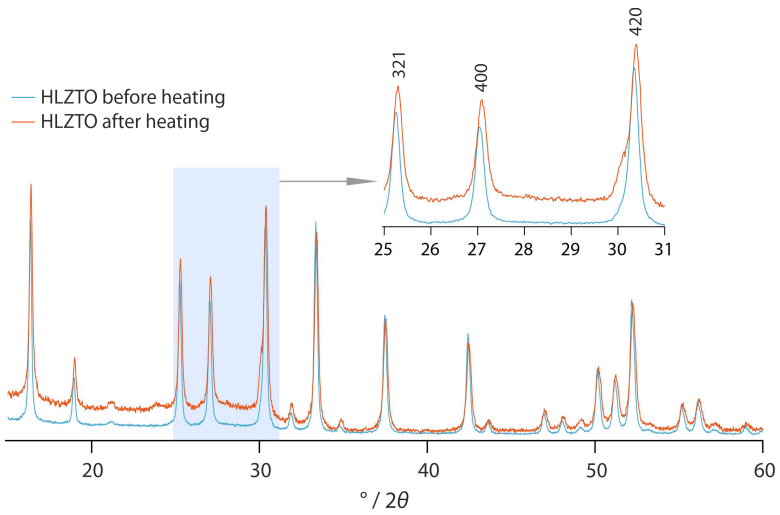

Figure S6: Comparison of the XRD patterns of HLZTO before and after exposure to 300 °C.

References

1. T. Scheiber, B. Gadermaier, M. Finsgar and H. M. R. Wilkening, *Adv. Funct. Mater.*, 2024, **34**.
2. S. Lunghammer, Q. Ma, D. Rettenwander, I. Hanzu, F. Tietz and H. M. R. Wilkening, *Chem. Phys. Lett.*, 2018, **701**, 147-150.
3. D. Tapler, B. Gadermaier, J. Spychala, F. Stainer, A. Marko, J. Königsreiter, K. Hogrefe, P. Heitjans and H. M. R. Wilkening, *J. Am. Chem. Soc.*, 2025, **147**, 20023-20032.